Experimental system and image analysis software for high throughput phenotyping of mycorrhizal growth response in *Brachypodium distachyon*

Felicia Maviane-Macia[1], Camille Ribeyre[1], Luis Buendia[1], Mégane Gaston[1], Mehdi Khafif[1], Fabrice Devoilles[1] Nemo Peeters[1,2]*, Benoit Lefebvre[1,2]*

[1]LIPM, Université de Toulouse, INRA, CNRS, Castanet-Tolosan, France

[2]These authors contributed equally to this work

*authors for correspondence, e-mail: benoit.lefebvre@inra.fr; telephone 0033+(0) 5 61 28 53 22, nemo.peeters@inra.fr; telephone 0033+(0) 5 61 28 55 92

ORCID:

Felicia Maviane-Macia : 0000-0002-4217-7707

Luis Buendia: 0000-0002-9511-6334

Nemo Peeters: 0000-0002-1802-0769

Benoit Lefebvre: 0000-0002-3810-605X

Total word count for the main body of the text: 4805 words

Introduction: 727 words

Results: 1549 words

Discussion: 1843 words

Materials and methods: 665 words

5 figures(2 colour figures: fig. 1 and 2)

7 supplementary figures + 2 supplementary files

Abstract

- Plant growth response to Arbuscular Mycorrhizal (AM) fungi is variable and depends on genetic and environment factors that still remain largely unknown. Identification of these factors can be envisaged using high-throughput and accurate plant phenotyping.
- We setup experimental conditions based on a two-compartment system allowing to measure *Brachypodium distachyon* mycorhizal growth response (MGR) in an automated phenotyping greenhouse. We developed a new image analysis software "*IPSO Phen*" to estimate of *B. distachyon* aboveground biomass.
- We found a positive MGR in the *B. distachyon* Bd3-1 genotype inoculated with the AM fungi *Rhizophagus irregularis* only if nitrogen and phosphorus were added together in the compartment restricted to AM fungi. Using this condition, we found genetic diversity in *B. distachyon* for MGR ranging from positive to negative MGR depending on the plant genotype tested.
- Our result on the interaction between nitrogen and phosphorus for MGR in *B. distachyon* opens new perspectives about AM functioning. In addition, our open-source software allowing to test and run image analysis parameters on large amount of images generated by automated plant phenotyping facilities, will help to screen large panels of genotypes and environmental conditions to identify the factors controlling the MGR.

Five to eight key words

Automated plant phenotyping, Image-analysis software, Arbuscular Mycorrhizal symbiosis, *Brachypodium distachyon*, nutrition, phosphate, nitrate, ammonium

Introduction

Arbuscular mycorrhiza (AM) is one of the most ancient plant-microorganism mutualist symbiosis that occurs between most plant species and Glomeromycota fungi. It is commonly accepted that AM can lead to a better plant growth (Smith & Read, 2008). The extended mycelium network in soil enables the fungi to uptake macro- and micronutrients in areas that are not exploited by plants roots. These nutrients are then transported through the mycelium to the roots and exchanged with plant metabolites (carbohydrates and lipids). Both nitrogen (N) and phosphorus (P), the most limiting nutrients for plant growth can be provided to plants (Pearson & Jakobsen, 1993; Tobar *et al.*, 1994; Smith *et al.*, 2004; Govindarajulu *et al.*, 2005; Fellbaum *et al.*, 2014). AM fungi have both nitrate and ammonium transporters and can thus uptake these two N-containing ions from the soil (reviewed in Chen *et al.*, 2018). Consequently AM plays a key role in plant nutrition in natural ecosystems and in low fertilization agricultural systems in which the soil N and P availability is often limiting for plant growth.

However, there is host and symbiont genetic variability for plant growth stimulation by AM fungi in controlled conditions. For example, mycorrhizal growth response (MGR) can be either positive or negative in wheat (Hetrick & Wilson, 1992; Xavier & Germida, 1998; Lehnert *et al.*, 2018) and sorghum (Watts-Williams *et al.*, 2019). Very little is known about the genetic determinants that control MGR. Identification of the underlying plant loci/genes is a major scientific challenge and would help to breed crops for improved MGR and increased performance in low fertilization agriculture.

Genetic studies to identify such loci/genes require high-throughput and accurate plant phenotyping in the presence or absence of the AM fungi. We test the feasibility of such genetic studies on *Brachypodium distachyon*, using an automated phenotyping platform (the "Toulouse Plant-Microbe Phenotyping" or "TPMP" facility).

B. distachyon is a wild Mediterranean diploid grass with a relatively small size and short cycle (Girin *et al.*, 2014). Variability of *B. distachyon* MGR to various AM fungal genotypes has been shown (Hong *et al.*, 2012) but host genetic effect on MGR has not been studied yet.

Effect of AM on plant growth is highly dependent on environmental conditions and in particular on nutrient availability in the soil. Plant colonization by AM fungi is also regulated

by nutrient availability (Bonneau *et al.*, 2013; Nouri *et al.*, 2014). Thus controlling soil nutrient availability is critical to study MGR. We used a two-compartment system, one of them being only accessible to AM fungi and supplemented with N and/or P, to mimic the ability of AM fungi to collect these nutrients in large soil volumes that cannot be explored by the plant root. A compartment only accessible to AM fungi was used to demonstrate N and P transport in plants using $^{32}P/^{33}P$ or ^{15}N (Pearson & Jakobsen, 1993; Tobar *et al.*, 1994; Smith *et al.*, 2004; Govindarajulu *et al.*, 2005; Fellbaum *et al.*, 2014). However, the effect of the nature and amount of nutrients in the compartment restricted to AM fungi, and particularly of combination of N and P, on MGR, remains to be determined.

Plant aboveground biomass can be estimated in a fast and non-destructive way by image analysis. In *B. distachyon,* this biomass was found to be well correlated with the shoot "biovolume" (Poire *et al.*, 2014).

Image segmentation can be performed by chaining various image processing tools in a pipeline. Creation of pipelines and/or adjustment of each tool parameters is required to set-up segmentation of images captured by camera on phenotyping platforms. There are many freely available Image processing libraries or programs, but to our knowledge none that has a user interface, can generate pipelines that can be rapidly tested on defined image subsets and apply the analysis pipelines on large amount of image data.

Here we describe an experimental system based on a two-compartment system allowing the measurement of *B. distachyon* MGR using a state-of-the-art high-throughput phenotyping facility. We show that both N and P mobilization by the AM fungi is critical for MGR in *B. distachyon* and that there is genetic variability in *B. distachyon* for MGR. We also provide a new Python-based software tool called "*IPSO Phen*". This open-source tool allows to configure and test image processing tools embedded in pipelines that can be executed on large amount of images generated by automated plant phenotyping facilities.

Results

Access of AM fungi to nitrogen and phosphorus is required for positive mycorrhizal growth response in B. distachyon

Our first goal was to design an experimental system allowing measurement of MGR in B. *distachyon* grown in pots. To control the nutrient availability for the plant and the AM fungi,

we used a 1:1 (v/v) mixture of calcinated-clay and sand as substrate. To mimic the fact that *in natura* AM fungi can access nutrients that are not available to the plant roots, we use a two-compartment system. A plastic tube covered by a nylon mesh (hyphal compartment, HC), fine enough to exclude plant roots but not the AM fungal hyphae, was filled with calcinated-clay supplemented with N and/or P and placed at the bottom of 3L pots (Fig. 1a). Since N is a diffusible nutrient, part of the N can diffuse out of the HC and be accessible to plant roots. In order to limit this effect, we made sure that the total quantity of N introduced in the HC corresponds to the reported need for *B. distachyon* optimal growth (David *et al.*, 2019). As P is not diffusible and would thus not leach out the HC, it was put in excess. When no N and P were supplemented in the HC, they were provided to the plants as phosphate directly mixed in the soil or nitrate through a nutritive solution.

In order to test the effect of N and/or P in the HC on *B. distachyon* growth, seedlings of the *B. distachyon* genotype Bd3-1 were inoculated with or without spores of the AM fungal species *Rhizophagus irregularis* and grown for 4 weeks in a growth chamber. Some plants were harvested to determine by microscopy the level of fungal colonization in roots. At 4 weeks post inoculation (wpi), in average, 32% of each root system was colonized by AM fungi. No colonization was found in non-inoculated plants. The left over plants were grown for an extra 8 weeks in an automated greenhouse (Fig. S1a). At the end of the experiment (12 wpi), in average, 56% of each root system was colonized by AM fungi. Aboveground dry weights were also measured. A significant increase in Bd3-1 aboveground biomass was observed in mycorrhizal plants only when the HC was supplemented with a mixture of phosphate, ammonium and nitrate (Fig. 1b). Similar positive MGR on Bd3-1 was observed using sand alone as a substrate (Fig. S2).

This result shows that it is possible to establish a mutualistic symbiosis between *B. distachyon* genotype Bd3-1 and *R. irregularis* in controlled conditions, but only when AM fungi have access to a source of N and P.

"ISPO phen", a Python-based software tool, enables a fast setup and test of image processing pipelines for optimized segmentation and feature extraction

Instead of measuring aboveground dry weight, we aimed to estimate plant aboveground biomass through image analysis. This required segmentation of the plant pixels over the

background. This can be easily done for a limited number of plants using freely-available analysis tools popular among the plant phenotyping community, namely ImageJ (Rueden *et al.*, 2017) and the Python based Scikit-image (van der Walt *et al.*, 2014), OpenCV (Bradski. 2000) or PlantCV (Gehan *et al.*, 2017). However, users are required to adjust image processing tool settings individually and tests must be done manually, which is time consuming. The procedure of setting and testing pipeline items in sets containing large amount of images can easily become cumbersome. Plant high-throughput phenotyping generates large amount of image data. Here each plant is imaged daily (8 images with a 45° angle between each imaged, Fig. S1b) over a two-month period (60 days). Considering the 264 pots as the maximal set up possible in the phenotyping greenhouse 2 of our facility (Fig. S1a), one such experiments could generate up to 8x60x264= 126 720 images. Our goal was to optimize the high-throughput segmentation of the plant pixels. Important features that we thought to be essential for this are the possibility to : (i) rapidly and semi-automatically test the solution space of given segmentation parameters, (ii) generate and test analysis pipelines, (iii) apply analysis pipelines on large amount of image data. As these features are not well served by the existing tools, we set out to develop "*IPSO phen*" a software built with Python using OpenCV, numpy (van der Walt *et al.*, 2011), pandas (McKinney, 2010) and Scikit-image. *IPSO phen* also includes a user interface, access to image database and the possibility to create or import new tools, including some tools already developed in PlantCV for instance. The *IPSO phen* documentation (https://ipso-phen.readthedocs.io/en/latest/installation.html) and the source code (https://github.com/tpmp-inra/ipso_phen) are freely available.

Fig. 2a displays the flow chart that was defined and applied on the *B. distachyon* side images generated in this work. *IPSO Phen* can the save pipelines as Python scripts (see supplementary files: pipeline_script.py or binary files: pipeline_binary.tipp) that can be used to restore the process or be modified to better suite one's needs.

Versatility of the "IPSO phen" segmentation pipeline for B. distachyon analysis

An important feature of an image analysis process is that it has to be capable of both handling large amount of data and be sufficiently versatile to cope with variation in the image features and quality. To illustrate this we choose to present the segmentation performance of the developed *IPSO phen* pipeline on small plantlets (Fig. S3a), larger and

flowering plants (Fig. S3b), images with line errors (Fig. S3c) and images where misplacement of the covering foam disc (Fig S3d). The line errors are the result of data transfer issues between the camera and the database, can affect up to 10% of the images on some given days. The foam discs misplacement can be from the initial installation or appear during the experimentation and are quite rare event. Although not so common this could not be ignored and the coarse mask addressed the issue. The biomass of both small plantlets (initial stages of growth) and cases of data transfer error and disc misplacements could thus be managed by the analysis pipeline and return usable data points. The images of larger, flowering plants was not used in this work, but the pipeline could readily exploit characteristic features of this development stage.

The addition of the tutor cages on top of the pots was required to avoid any *B. distachyon* tillers from falling (which some genotype have a tendency for) but added an extra segmentation challenge, not only due to the division of plant part in sectors defined by the cage structure, but also bringing some extra light reflexion. These cages also mask plant material, with a more pronounced effect on smaller plants. In order to have the best segmentation, we applied different tools to several region of interest (ROI) of the image (step 3 of pipeline Fig. 2a).

B. distachyon side image-determined "projected surface median" correlates with aboveground shoot biomass

We decided to calculate a proxy of plant shoot biomass by using side images. This proxy was generated for each plant imaging passage by calculating the median plant pixel number of 8 images taken at consecutive 45° angles. To determine whether this plant "median projected surface" (MPS hereafter) provided by image analysis correlate with the plant biomass over the *B. distachyon* growth cycle, we harvested *B. distachyon* plants weekly and measured both the MPS from images and the actual biomass. We found a good correlation (R^2=0.975) between the aboveground MPS and the aboveground dry weight (Fig. 3). The correlation was lost once the spikelets appeared (Fig. S4), showing that the MPS is a good approximation of shoot but not seed biomasses.

Image analysis shows that mycorrhizal growth response in B. distachyon depends on plant nutrition through AM fungi

We then applied image segmentation and MPS calculation to follow the growth kinetic of Bd3-1 in presence or absence of AM fungi (Fig. 4a). To quantify the effect of AM fungi on growth, we measured the "area under the curve" (AUC) for each individual (Fig. 4b) we also calculated the MGR using the MPS at the end of the cycle (Fig. 4c). Better plant growth was observed in presence of AM fungi when N and P were added in the HC and plant N/P fertilization was low. In this condition, a significant difference in the AUC was found between mycorrhizal and the non-mycorrhizal plants (Fig. 4b), leading to a positive MGR (Fig. 4c). Analysis of plant MPS at each day of the kinetic showed that a significant difference between mycorrhizal and the non-mycorrhizal plants appeared 45 days after inoculation with AM fungi (17 days after addition of the HC in the experimental system). In contrast, no significant increase in growth of mycorrhizal plant compared to non-mycorrhizal plants, was observed when no N and P were added to the HC and N/P fertilization was low (Fig. 4a-c). Similarly, when N and P were added to the HC but plants were fertilized with high levels of N and P, no effect of AM fungi on plant growth was observed (Fig. 4a-c).

To determine whether there is genetic variability in *B. distachyon* for MGR and whether our experimental conditions allows to measure it, we initiated a screen *B. distachyon* genetic diversity for MGR. Differences were observed between the 16 genotypes tested ranging from positive to negative MGR (Fig. 5).

Discussion

Plant automated high throughput phenotyping enables to have more data points for a plant trait of interest compared to classical human-recording phenotyping. These can be more individuals as well as more time points. Moreover, the automated phenotyping platform, including the watering facility, allows to decrease the experimental variability within a given experiment. We would like to emphasis that we observed in this work a very low growth variability between plants with the same treatment within each replicate. Although not quantifiable as such, this variability was much lower compared to what we observed in various experiments we ran previously in growth chambers or greenhouses (although the plants were not grown under the exact same condition). However, we observed a strong variability between the first/second and the third replicates when we analyzed the *B. distachyon* genetic variability for MGR. For an unexplained reason, in the third replicate all genotypes started to flower during the 4 weeks the plants were in the growth chamber while

the first spikelets started to appear 1 week after transfer in the greenhouse in the two first replicates. This had a strong effect on MGR although the type of effect (positive or negative MGR) was similar between the replicates. Moreover, the early flowering plants had a reduced growth that affected the quality of image-segmentation with the imaging parameters we selected for our experiments (Fig. S6). Low variability of growth between individuals was also observed previously and led to the successful phenotyping of other plant-microbe interactions (Mazo-Molina *et al.*, 2019). We thus believe that the plant rearing conditions in the TPMP facility (Fig. S1a) are quite homogeneous, minimizing the biological variability.

We chose to estimate the shoot biomass only using side images, and not a combination of side and top images like (Poire *et al.*, 2014). This was mainly due to a phenotyping time consideration, as the top and side imaging can't run simultaneously (lighting conditions are different). Top imaging would have implied a second phenotyping job, not compatible with other experiments running on the facility at the same time. However, the correlation with biomass was similar to that found in (Poire *et al.*, 2014). Moreover, the use of the median pixel plant number has the advantage of being quite tolerant to accidental variations (for instance a tiller that would be blocked in the tutor cage).

IPSO Phen a new opensource software allowing the fast development of pipelines for plant image segmentation

In this work we have developed a new software suite that we believe is well suited to the analysis of large amount of image data, typically generated by high throughput plant phenotyping. The most popular open-source solutions for analyzing large plant-phenotyping data is PlantCV (Gehan *et al.*, 2017). The clear advantages of PlantCV are (i) the fact that it is built on known image-analysis toolkits like OpenCV or Scikit-image, whilst being (ii) easier to use than OpenCV (iii) its opensource nature, and (iv) large user community. We believe that *IPSO phen* could be a good addition/companion to PlantCV. Indeed *IPSO phen* fills the gap of known drawback of PlantCV as it provides (i) a User Interface, (ii) doesn't require one to be a Python programmer, (iii) provides the possibility to build and test image processing pipelines as they are being built. Like PlantCV, *IPSO phen* is built on industry standards (OpenCV, Scikit-image, numpy and pandas), it is easily extendable as new tools and plugins can be created and/or added from known sources. We have imported popular PlantCV tools within

the tool kit available in *IPSO phen*, these tools (by convention; named PCV in *IPSO phen*), can readily be integrated and tested in any new pipeline. A grid search, allows to explore a wide solution space in a very simple way, with easy inspection and selection by the user of the desired tool settings. Finally, in our experiments, imaging was performed daily and the raw images where stored in a dedicated database (not discussed in this work). *IPSO phen* software also has the advantage to directly access the desired images in the database. In conclusion, *IPSO phen* is meant to be used for high throughput as it connects directly with image databases (or filesystem), the pipeline functions can be tested on fixed or random sets of images at every step and the mass processing can be done in various steps.

IPSO phen is fully functional, but still in its early development. A roadmap for the future would be an improvement of the User Interface and a more flexible and intuitive pipeline builder.

Co-transport of N and P might be required for efficient mycorrhizal growth response in B. distachyon

In our controlled conditions, *B. distachyon* growth stimulation by AM fungi was observed only when N and P were added in the HC accessible to the AM fungi. This suggests that the growth stimulation is due to plant N and P nutrition through the AM fungi. It has to be noted that the growth of *B. distachyon* was similar when N and P were transported through AM fungi (+ AM fungi, fertilization with low N and P in the pot) or directly acquired by the root system (- AM fungi, fertilization with high N and P in the pot). The lack of *B. distachyon* growth increase between the conditions in which N and P were added or not in the HC in absence of AM fungi suggests that diffusion of at least one the two nutrients is limited. The requirement of the presence of both N and P in the HC for positive MGR in *B. distachyon* was a surprising result. Indeed, positive MGR on maize was observed by introducing only P to the HC (Gerlach *et al.*, 2015). However, it might explain the absence or negative MGR observed in many experimental systems used in controlled conditions even if P transport from the HC to the plants was measured (Smith *et al.*, 2004; Li *et al.*, 2006). In our experimental system, when either only N or P were added in the HC, the other nutrient was added to the substrate outside of the HC and thus accessible to both AM fungi and roots. The lower plant growth compared to the condition in which both nutrients were added to the HC or directly in the substrate, suggests that uptake both nutrients is inefficient if not performed through the

297 same mechanism (direct uptake or through AM fungi). It has been hypothesized that N and P
298 can be co-transported in the AM fungal mycelium from the place they are collected to the
299 arbuscules in plant roots. N is transported as arginine and P as polyphosphate, and arginine
300 can bind to polyphosphate (Govindarajulu *et al.*, 2005). Stoichiometry of N and P in the
301 mycelium might thus affect efficiency of their transport. Alternatively, colonization of plants
302 by AM fungi can strongly repress expression of phosphate, nitrate and ammonium
303 transporters involved in direct nutrient uptake, including in *B. distachyon* (Hong *et al.*, 2012).
304 The P availability in the soil also interferes with N uptake and AM-dependent regulation of N
305 transporters (Nouri *et al.*, 2014). It could be that colonization by AM fungi induces repression
306 of direct nutrient uptake even if the AM fungi cannot provide all limiting nutrients for plant
307 growth. It should be determined to which extent availability of N, P or N+P in the HC affects
308 the direct uptake of both N and P.

309 Genes coding for both nitrate and ammonium transporters are found in AM fungi (reviewed
310 in Chen *et al.*, 2018). When in competition with nitrate, ammonium (provided as ammonium
311 nitrate in the HC) appeared to be the preferred N source for AM fungi, both in terms of
312 uptake by AM fungi and delivery to plants (Tanaka & Yano, 2005). However, when only
313 nitrate or ammonium were used as N sources (both for plant and AM fungi), better N
314 transport by AM fungi to plants was obtained with nitrate (Hawkins & George, 2001). The
315 authors suggested that pure ammonium can be deleterious for AM fungi. In our
316 experimental conditions, we found a positive MGR if ammonium and nitrate were added
317 together with P in the HC but not if only ammonium was added together with P, suggesting
318 that a balance between ammonium and nitrate is required for efficient N uptake by AM
319 fungi.

320 We observed positive MGR on the *B. distachyon* genotype Bd3-1 from 45 days after
321 inoculation and 17 days after addition of the HC. Once the HC was added to the pots, it
322 might take a few days for AM mycelium to reach the HC and start to uptake the nutrients it
323 contains. We have not observed significant growth depression in the mycorrhizal plants
324 before the AM fungi reach the HC and can provide a nutritional benefit. This suggests that in
325 our conditions the carbon cost of AM establishment is not limiting for plant growth or is
326 compensated by an increase of plant photosynthetic activity.

Here we show that AM fungi can stimulate the increase of *B. distachyon* shoot biomass. It would be interesting to determine which other plant traits are affected during AM. Image analysis can easily determine additional aboveground plant traits such as height, width, and various features of the aboveground plant shape. Automatic analysis of other traits such as the tiller number or the flowering time would require development of new pipelines/tools. In addition, seed development would be another important trait to follow. It would be interesting to analyze whether any changes in imaging variables correlate with effects of AM fungi on seed quantity and/or quality and could be used as proxy to follow effects of AM on seed production.

Testing MGR in 16 *B. distachyon* genotype, we observed variability between genotypes, ranging from a positive to negative MGR. Reasons that can explain host genetic variability for MGR are not known. Differences in host efficiency to acquire N and P from AM fungi could be one of them. Alternatively, AM fungi induce plant defense (Güimil *et al.*, 2005; Campos-Soriano *et al.*, 2012; Watts-Williams *et al.*, 2019) and trade-off between plant growth and defense are known (reviewed in Karasov *et al.*, 2017). Differences in level of host defense induction by AM fungi might explain difference in MGR. The genetic variability observed in *B. distachyon* is similar to that observed in other species except in maize for which only positive MGR were found (Kaeppler *et al.*, 2000; Sawers *et al.*, 2017). It is interesting to note that in maize, positive MGR was also found when only P was added in the HC. Together it suggests that both nutrition (direct nutrient uptake and/or through AM fungi) and MGR are different in maize and *B. distachyon* or other grass species.

Identification of plant loci/genes controlling MGR would be of interest to help breeding for optimized MGR. The experimental design we setup, the genetic variability we found in *B. distachyon* and the software we developed for high throughput image analysis make feasible analysis of MGR on large panels of *B. distachyon* accessions / recombinant lines and quantitative genetics allowing identification such gene/loci in this species.

Materials and methods

Plant growth conditions

Brachypodium distachyon Bd3-1 was used for setting up the experimental system. Variability of mycorrhizal growth responses was tested on the other indicated genotypes. Seeds were

surface sterilized for 30 sec in 70% ethanol and for 5 minutes in 3.2% active chlorine bleach solution. Seeds were placed in agar plates and incubated at 1 week (Bd3-1, Bd21, and Bd21-3) or 4 weeks (the other genotypes) at 4° C. The seeds were germinated for 3 days at 25°C before planting.

Seedlings were planted in peat pots (Fig. S7a) filled with about 250 ml of a 1:1 (v/v) mix of calcinated clay (Attapulgite Sorbix) and quartz sand (0.7-1.3 mm) and inoculated with 2000 spores of *Rhizophagus irregularis* DAOM 197198 (Agronutrition, France).

Plantlets were grown for 4 weeks in a growth chamber (16h of light, LED light at 300 µmol.m^{-2}.s^{-1}, 24 °C - 8h of dark, 18 C). Each pot was individually watered with the same volume of a low N and P nutritive solution 3 times per week (Table S1). After 4 weeks, each peat pot was placed in a 3L plastic pot (3LSX, Bleu EK, Soparco, France) filled with the same substrate. A 40 ml plastic container filled with the calcinated clay and covered by a 30 µm nylon mesh was used as hyphal compartment (HC). The HC was supplemented with 305mg of NH_4Cl, 577mg of KNO3, or 130 mg of KNO_3+177 mg of NH_4NO_3 (each condition corresponding to 80 mg of N) and/or 115 mg of KH_2PO_4. The HC was placed at the bottom of the 3L pots. For the high N and P condition, 25ml of the N solution (10 mM KNO_3 and 10 mM $Ca(NO_3)_2$) were added weekly and/or 115mg of KH_2PO_4 were mixed with the substrate used to fill the 3L pots, once the 3L pots were loaded on the automated greenhouse. A blue foam disc (eva/rubber composition, 210 g.m^{-2}, 2mm thick, uniform blue colour) was glued on the rim of the pots to facilitate image segmentation (Fig. S7b). These discs also have the advantage of guiding the watering flow towards the center of the pot and lowering water loss by soil evaporation. A blue tutor cage (Sopafix 19 BAS, Bleu EK, Soparco, France) was attached on each pot to maintain all plant tillers upwards and thus allow more reproducible plant imaging (Fig. S7c). Plants were grown on the automated greenhouse (Fig. S7d) with watering three times per week with 8 ml of 2.5x nutritive solution (Table S1). Additional water was added to maintain each pot at a fixed weight corresponding to 70% of the maximal water retention capacity.

For measuring the correlation between image analysis and aboveground dry weight, Bd3-1 seedling were planted on potting soil (SB2, Proveen, The Netherlands) supplemented with 1.7g/L of osmocote (12-7-19+TE) and grown on the automated greenhouse. Four plants were harvested weekly.

IPSO phen

The documentation files are available through readthedocs (https://ipso-phen.readthedocs.io/en/latest/installation.html) and contains all the details and explanation of how to install and use *IPSO phen*. The software was built using OpenCV (Gehan *et al.*, 2017), numpy (van der Walt *et al.*, 2011), pandas (McKinney, 2010) and Scikit-image (van der Walt *et al.*, 2014). The source files are available through Github (https://github.com/tpmp-inra/ipso_phen). *IPSO phen* was created to (i) have a user interface, (ii) build for high throughput (image database connection, functions can be tested at each step, mass process in various steps) (iii) new tools/plugins can be added or built (declarative UI building, callbacks handled behind the scene, documentation and docstrings built automatically), (iv) Grid search to explore solution space in single process. Specific inquiries can be made using the dedicated email address: ipsophen@inra.fr

Data analyses

Growth curve regressions were calculated using geom_smooth from R's tidyverse library with method "loess" and "y ~ x" formula. Areas under the curves were measured using the script audpc in the R library agricolae. Statistical differences in the aboveground dry weights, plant MPS at the fixed days or AUC were analyzed using a Kruskal Wallis test ($p<0.05$).

Acknowledgements

Seeds were kindly provided by Richard Sibout (INRA, France) and John Vogel (DOE-JGI, USA).

Author contributions

BL and NP designed and planned the experiments. FMM designed and created *IPSO phen* software. CR, LB, MG, MK, FD performed the experiments. FMM, NP and BL analyzed the data. FMM, NP and BL wrote the manuscript.

Funding information: This work was supported by the "Laboratoire d'Excellence (LABEX)" TULIP (ANR-10-LABX-41) and by the Institut carnot "Plant2Pro" (contracts STRESSNSYM and PHENOR).

Supporting Information :

Fig. S1. Phenotyping system design.
Fig. S2. AM fungi access to N and P is required to stimulate Bd3-1 growth of in controlled conditions.
Fig. S3. *IPSO phen* pipeline versatility.
Fig. S4. *B. distachyon* seed biomass cannot be estimated by side image segmentation.
Fig. S5. Growth of 16 *B. distachyon* genotypes in presence or absence of *R. irregularis*.
Fig. S6. Normalized growth of 16 *B. distachyon* genotypes in presence or absence of *R. irregularis*.
Fig. S7. Experimental system design.
Supplementary file 1: pipeline_script.py
Supplementary file 2: pipeline_binary.tipp

References

Bonneau L, Huguet S, Wipf D, Pauly N, Truong HN. 2013. Combined phosphate and nitrogen limitation generates a nutrient stress transcriptome favorable for arbuscular mycorrhizal symbiosis in Medicago truncatula. *New Phytol* **199**: 188-202.

Bradski G. 2000. The opencv library. *Doctor Dobbs Journal* **25**:120-126

Campos-Soriano L, Garcia-Martinez J, Segundo BS. 2012. The arbuscular mycorrhizal symbiosis promotes the systemic induction of regulatory defence-related genes in rice leaves and confers resistance to pathogen infection. *Mol Plant Pathol* **13**: 579-592.

Chen A, Gu M, Wang S, Chen J, Xu G. 2018. Transport properties and regulatory roles of nitrogen in arbuscular mycorrhizal symbiosis. *Semin Cell Dev Biol* **74**: 80-88.

David LC, Girin T, Fleurisson E, Phommabouth E, Mahfoudhi A, Citerne S, Berquin P, Daniel-Vedele F, Krapp A, Ferrario-Méry S. 2019. Developmental and physiological responses of Brachypodium distachyon to fluctuating nitrogen availability. *Sci Rep* **9**: 3824.

Fellbaum CR, Mensah JA, Cloos AJ, Strahan GE, Pfeffer PE, Kiers ET, Bücking H. 2014. Fungal nutrient allocation in common mycorrhizal networks is regulated by the carbon source strength of individual host plants. *New Phytol* **203**: 646-656.

Gehan MA, Fahlgren N, Abbasi A, Berry JC, Callen ST, Chavez L, Doust AN, Feldman MJ, Gilbert KB, Hodge JG, et al. 2017. PlantCV v2: Image analysis software for high-throughput plant phenotyping. *PeerJ* **5**: e4088.

Gerlach N, Schmitz J, Polatajko A, Schluter U, Fahnenstich H, Witt S, Fernie AR, Uroic K, Scholz U, Sonnewald U, et al. 2015. An integrated functional approach to dissect systemic responses in maize to arbuscular mycorrhizal symbiosis. *Plant Cell Environ* **38**: 1591-1612.

Girin T, David LC, Chardin C, Sibout R, Krapp A, Ferrario-Méry S, Daniel-Vedele F. 2014. Brachypodium: a promising hub between model species and cereals. *J Exp Bot* **65**: 5683-5696.

Govindarajulu M, Pfeffer PE, Jin H, Abubaker J, Douds DD, Allen JW, Bücking H, Lammers PJ, Shachar-Hill Y. 2005. Nitrogen transfer in the arbuscular mycorrhizal symbiosis. *Nature* **435**: 819-823.

Güimil S, Chang HS, Zhu T, Sesma A, Osbourn A, Roux C, Ioannidis V, Oakeley EJ, Docquier M, Descombes P, et al. 2005. Comparative transcriptomics of rice reveals an ancient pattern of response to microbial colonization. *Proc Natl Acad Sci U S A* **102**: 8066-8070.

Hawkins HJ, George E. 2001. Reduced N-15-nitrogen transport through arbuscular mycorrhizal hyphae to Triticum aestivum L. supplied with ammonium vs. nitrate nutrition. *Annals of Botany* **87**: 303-311.

Hetrick BAD, Wilson GWT. 1992. Mycorrhizal dependence of modern wheat cultivars and ancestors: A synthesis. *Can J Bot* **70**: 2032-2040.

Hong JJ, Park YS, Bravo A, Bhattarai KK, Daniels DA, Harrison MJ. 2012. Diversity of morphology and function in arbuscular mycorrhizal symbioses in Brachypodium distachyon. *Planta* **236**: 851-865.

Kaeppler SM, Parke JL, Mueller SM, Senior L, Stuber C, Tracy WF. 2000. Variation among maize inbred lines and detection of quantitative trait loci for growth at low

phosphorus and responsiveness to arbuscular mycorrhizal fungi. *Crop Science* **40**: 358-364.

Karasov TL, Chae E, Herman JJ, Bergelson J. 2017. Mechanisms to Mitigate the Trade-Off between Growth and Defense. *Plant Cell* **29**: 666-680.

Lehnert H, Serfling A, Friedt W, Ordon F. 2018. Genome-Wide Association Studies Reveal Genomic Regions Associated With the Response of Wheat. *Front Plant Sci* **9**: 1728.

Li HY, Smith SE, Holloway RE, Zhu YG, Smith FA. 2006. Arbuscular mycorrhizal fungi contribute to phosphorus uptake by wheat grown in a phosphorus-fixing soil even in the absence of positive growth responses. *New Phytol* **172**: 536-543.

Mazo-Molina C, Mainiero S, Hind S, Kraus C, Vachev M, Maviane-Macia F, Lindeberg M, Saha S, Strickler S, Feder A, et al. 2019. The Ptr1 Locus of Solanum lycopersicoides Confers Resistance to Race 1 Strains of Pseudomonas syringae pv. tomato and to Ralstonia pseudosolanacearum by Recognizing the Type III Effectors AvrRpt2 and RipBN. *Mol Plant Microbe Interact* **32**: 949-960.

McKinney W. 2010. Data structures for statistical computing in python. In: Proceedings of the 9th Python in Science Conference. SciPy Austin, TX. 51-56

Nouri E, Breuillin-Sessoms F, Feller U, Reinhardt D. 2014. Phosphorus and nitrogen regulate arbuscular mycorrhizal symbiosis in Petunia hybrida. *PLoS One* **9**: e90841.

Pearson J, Jakobsen I. 1993. The relative contribution of hyphae and roots to phosphorus uptake by arbuscular mycorrhizal plants, measured by dual labeling with P-32 AND P-33. *New Phytol* **124**: 489-494.

Poire R, Chochois V, Sirault XRR, Vogel JP, Watt M, Furbank RT. 2014. Digital imaging approaches for phenotyping whole plant nitrogen and phosphorus response in Brachypodium distachyon. *J Integr Plant Biol* **56**: 781-796.

Rueden CT, Schindelin J, Hiner MC, DeZonia BE, Walter AE, Arena ET, Eliceiri KW. 2017. ImageJ2: ImageJ for the next generation of scientific image data. *BMC Bioinformatics* **18**: 529.

Sawers R, Svane S, Quan C, Gronlund M, Wozniak B, Gebreselassie M, Gonzalez-Munoz E, Montes R, Baxter I, Goudet J, et al. 2017. Phosphorus acquisition efficiency in arbuscular mycorrhizal maize is correlated with the abundance of root-external hyphae and the accumulation of transcripts encoding PHT1 phosphate transporters. *New Phytol* **214**: 632-643.

Smith S, Read D. 2008. Mycorrhizal Symbiosis, 3rd Edition. *New York: Academic Press.*: 1-787.

Smith S, Smith F, Jakobsen I. 2004. Functional diversity in arbuscular mycorrhizal (AM) symbioses: the contribution of the mycorrhizal P uptake pathway is not correlated with mycorrhizal responses in growth or total P uptake. *New Phytol* **162**: 511-524.

Tanaka Y, Yano K. 2005. Nitrogen delivery to maize via mycorrhizal hyphae depends on the form of N supplied. *Plant Cell Environ* **28**: 1247-1254.

Tobar R, Azcon R, Barea J. 1994. Improved nitrogen uptake and transport from N-15-labeled nitrate by external hyphae of arbuscular mycorrhiza under water-stressed conditions. *New Phytol* **126**: 119-122.

van der Walt S, Colbert S, Varoquaux G. 2011. The NumPy Array: A Structure for Efficient Numerical Computation. *Comput Sci Eng* **13**: 22-30.

van der Walt S, Schönberger JL, Nunez-Iglesias J, Boulogne F, Warner JD, Yager N, Gouillart E, Yu T, contributors s-i. 2014. scikit-image: image processing in Python. *PeerJ* **2**: e453.

517 **Watts-Williams SJ, Emmett BD, Levesque-Tremblay V, MacLean AM, Sun X, Satterlee JW,**
518 **Fei Z, Harrison MJ. 2019.** Diverse Sorghum bicolor accessions show marked variation
519 in growth and transcriptional responses to arbuscular mycorrhizal fungi. *Plant Cell*
520 *Environ* **42**: 1758-1774.
521 **Xavier LJC, Germida JJ. 1998.** Response of spring wheat cultivars to Glomus clarum NT4 in a
522 P-deficient soil containing arbuscular mycorrhizal fungi. *Can J Soil Sci* **78**: 481-484.

Figure legends

Figure 1. AM fungi access to N and P is required to stimulate Bd3-1 growth of in controlled conditions. a) Schematic representation of the experimental system. One plant was grown per 3L pot. A tube separated by a nylon mesh (hyphal compartment, HC, red) and containing various sources of N and/or P nutrients was placed at the bottom de the 3L pot. AM fungi (orange) but not the roots (black) accessed to the N and P in the HC. b) Indicated N or P (KH_2PO_4) sources were put in the HC. Plant aboveground parts were harvested 12 wpi and dry weight (DW) were measured. Mycorrhizal Growth Response (MGR) was calculated as (mean DW of inoculated plants – mean DW of non-inoculated plants) / mean DW of non-inoculated plants. * indicates a significant difference in DW between inoculated and non-inoculated plants. n=4 individuals (from one biological replicate).

Figure 2: *IPSO phen* allows fast creation of pipelines to estimate *B. distachyon* aboveground biomass from side view images. a) Schematic representation of the pipeline used for *B. distachyon* image segmentation. b) Example of image processing at various steps of the pipeline (only steps 1, 2, 4, 5, 8 and 9 are illustrated). Numbers correspond to the step indicated in a). 1: **source image**, presence of a surrounding tutor cage, presence of reflection and diffraction noise. 2: **white balance and exposure**. This will fix any white balance or exposure errors that occurred during acquisition and will simplify comparisons as all images will have the same settings. 3: **Regions of interest** (ROI), this can be done manually or automatically, the types of ROI used here were the following: (i) keep ROI, everything outside will be deleted. (ii) safe ROI, contours inside this section won't be treated as strictly as those outside. (iii) open ROI, a morphology open operation (erode + dilate) will be applied inside. (iv) enforcer ROI, checks that the object is where it's supposed to be. 4: any **transformations** that renders segmentation easier, for this analysis we choose to replace the colour of darker and lighter as well as dominantly blue zones. Modification made at this step are not considered when images features are extracted 5: building **coarse masks**; in this pipeline a maximum of three coarse masks are needed: a mask to remove the tutor cage, a mask to remove the background, and another to remove the sensor noise. 6: **Merge Masks**, coarse masks as merged using logical operators "AND", or "OR" depending on the mask. 7: **Apply ROIs**, "keep", "delete" and "morphology" ROIs are applied at this step. 8: **Clean**

554 **Coarse mask**, clean the coarse mask defined at step 5. 9: **extract features** according to the
555 phenotyping question, here the projected plant pixels of each angle/image. For more
556 information, see readthedocs (https://ipso-phen.readthedocs.io/en/latest/installation.html).

557

558 **Figure 3. *B. distachyon* aboveground shoot biomass can be estimated by side image**
559 **segmentation.** Plot of the aboveground MPS and dry weights. The MPS is the median of the
560 plant pixel number obtained from the 8 images taken with 45° angles. Plants were harvested
561 weekly and the MPS was determined on images taken immediately before harvesting.

562

563 **Figure 4. Image segmentation allows to measure mycorrhizal growth response in Bd3-1.** a)
564 Growth curves of Bd3-1 in presence (+AMF) or absence (-AMF) of *R. irregularis* grown in pots
565 with HC containing N and P (+NP) or not (-NP). Plants were fertilized with low levels of N and
566 P (LNP) or high levels of N and P (HNP). n=4 individuals (from one biological replicate). b)
567 Differences in growth were quantified as areas under the curves (AUC). Different letters
568 represent statistically different categories. c) Mycorrizal Growth Response (MGR) was
569 calculated using the plant MPS at the end of the growth as (mean MPS of inoculated plants –
570 mean MPS of non-inoculated plants) / mean MPS of non-inoculated plants.

571

572 **Figure 5. Image segmentation allows to screen *B. distachyon* genetic variability for**
573 **mycorrhizal growth responses.** Plants were grown in presence or absence of *R. irregularis*
574 grown in pots with HC containing N and P and were fertilized with low levels of N and P. n=3
575 individuals (from 3 biological replicates). Mycorrizal Growth Response (MGR) was calculated
576 as log10 (MPS of inoculated plants / MPS of non-inoculated plants) in each biological
577 replicate using the plant MPS at the end of the growth. Triangles, Dots and squares
578 represent MGR in biological replicate 1, 2 and 3 respectively.

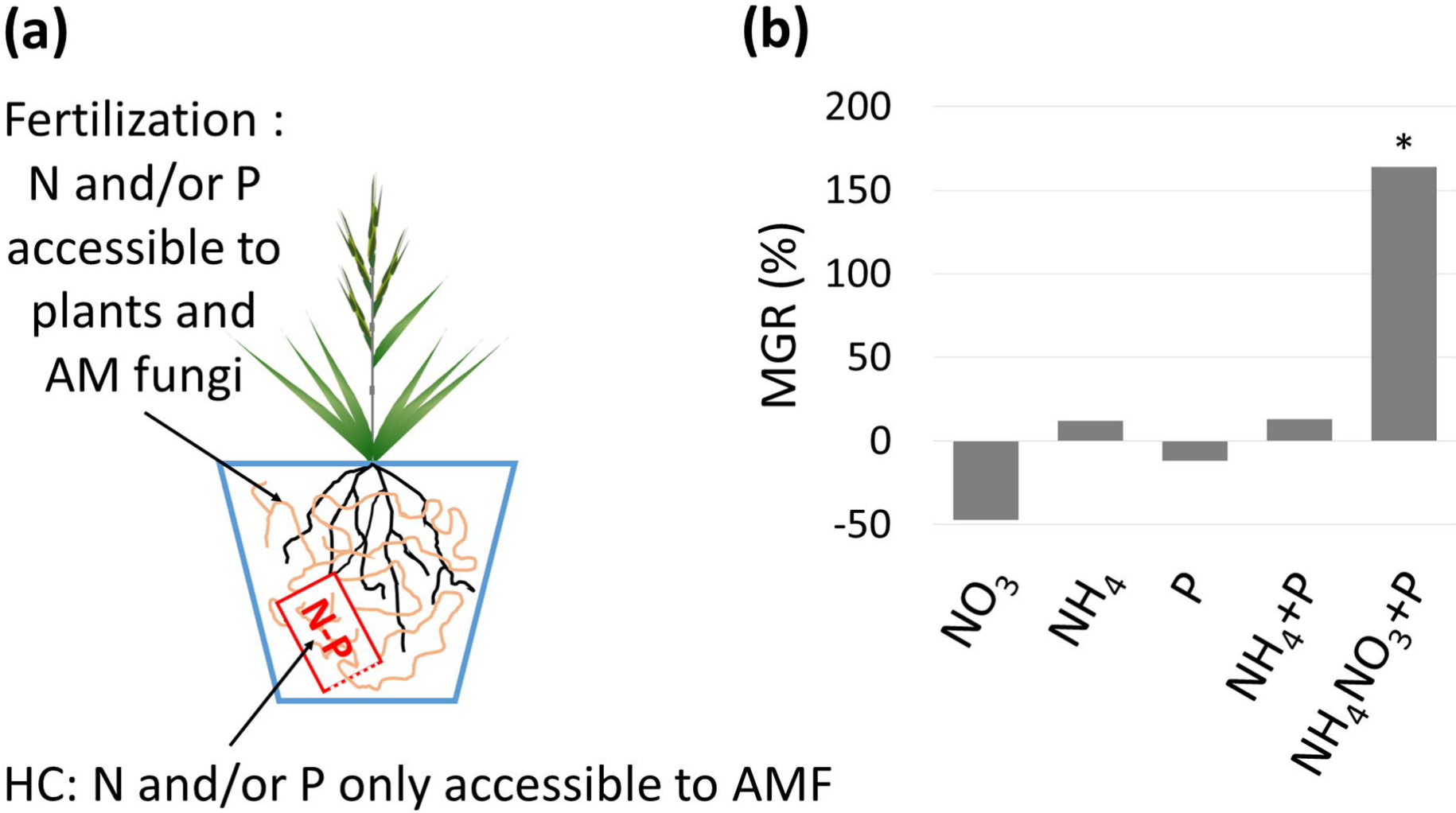
(a)
Fertilization :
N and/or P
accessible to
plants and
AM fungi
N-P
HC: N and/or P only accessible to AMF
(b)
MGR (%)
200
150
100
50
0
-50
*
NO3
NH4
P
NH4+P
NH4NO3+P

Figure 1

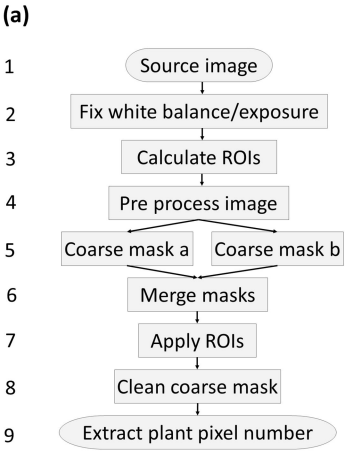
(a)
1
Source image
2
Fix white balance/exposure
3
Calculate ROIs
4
Pre process image
5
Coarse mask a
Coarse mask b
6
Merge masks
7
Apply ROIs
8
Clean coarse mask
9
Extract plant pixel number

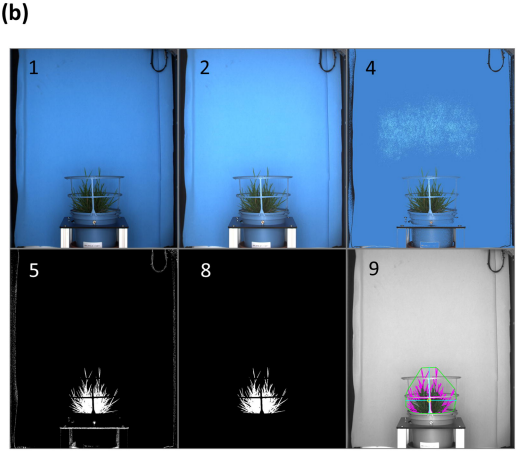
(b)
1
2
4
5
8
9

Figure 2

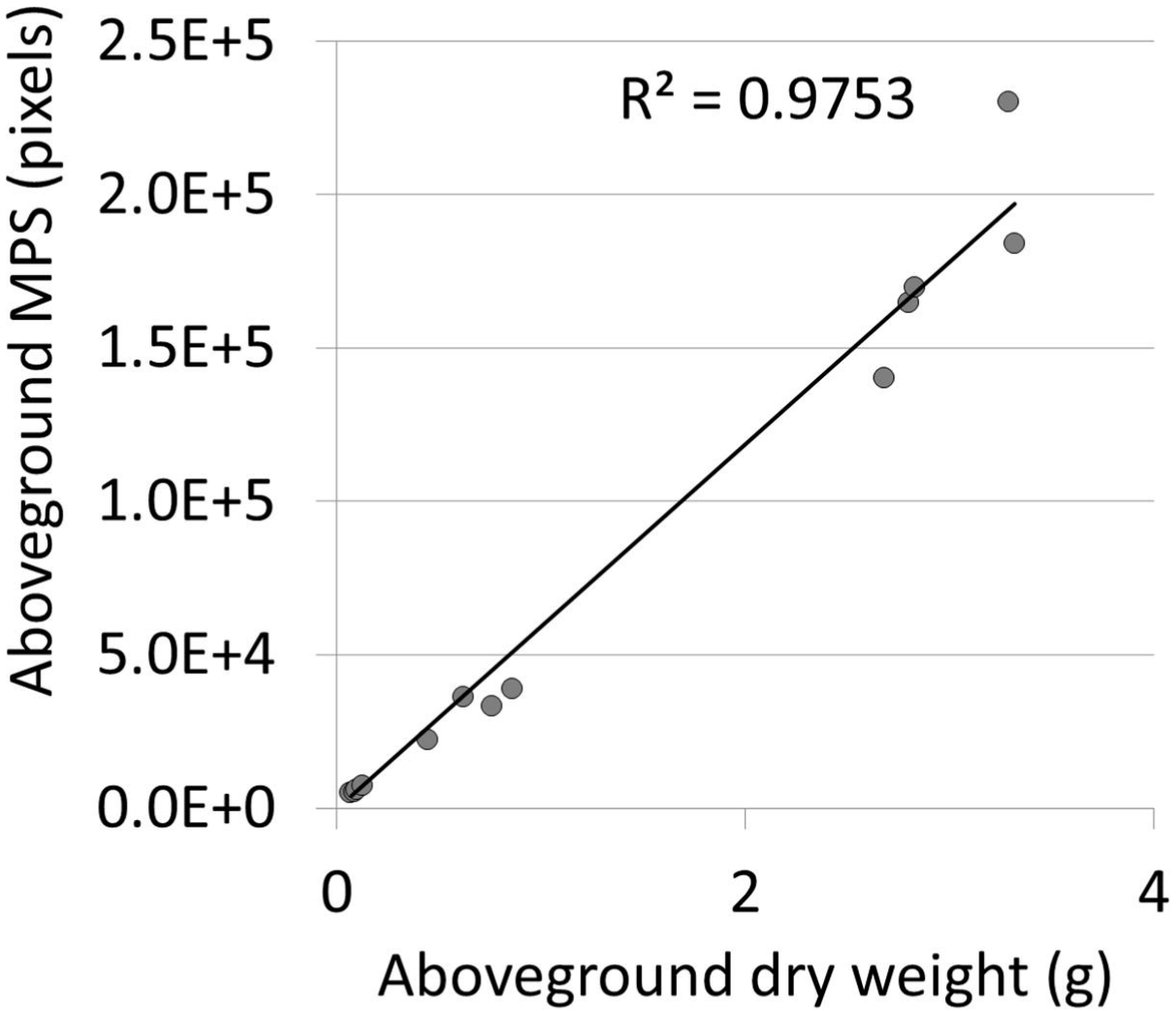
Aboveground MPS (pixels)
2.5E+5
2.0E+5
1.5E+5
1.0E+5
5.0E+4
0.0E+0
R² = 0.9753
0
2
4
Aboveground dry weight (g)

Figure 3

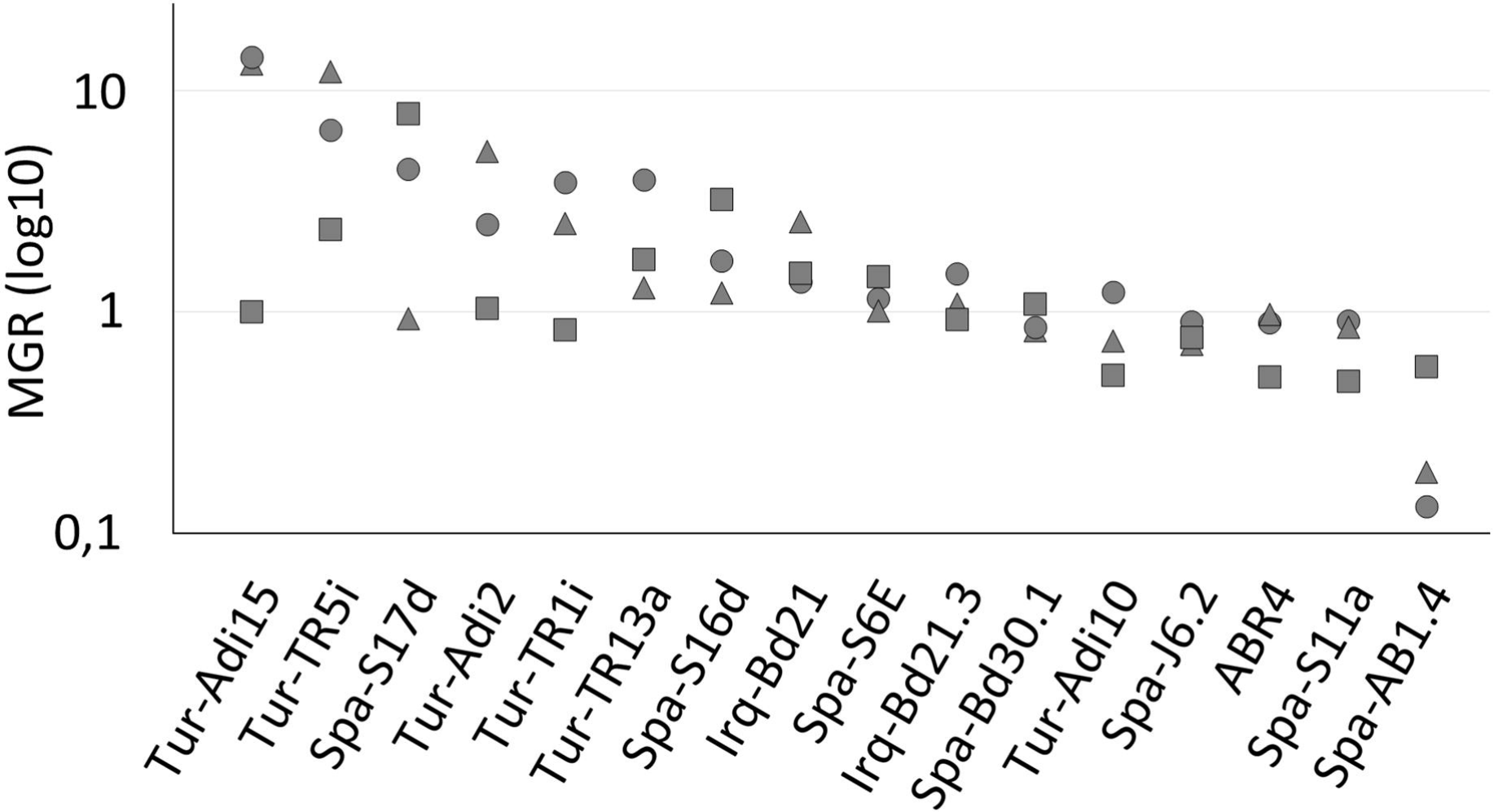
MGR (log10)
10
1
0,1
Tur-Adi15
Tur-TR5i
Spa-S17d
Tur-Adi2
Tur-TR1i
Tur-TR13a
Spa-S16d
Irq-Bd21
Spa-S6E
Irq-Bd21.3
Spa-Bd30.1
Tur-Adi10
Spa-J6.2
ABR4
Spa-S11a
Spa-AB1.4

Figure 5

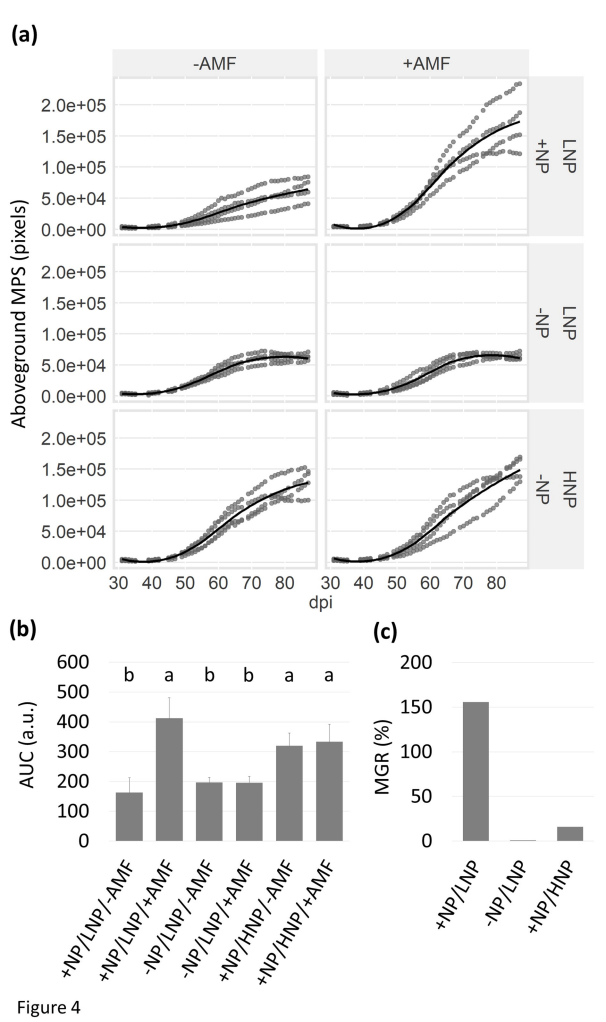
(a)
-AMF
+AMF
LNP +NP
LNP -NP
HNP -NP
Aboveground MPS (pixels)
2.0e+05
1.5e+05
1.0e+05
5.0e+04
0.0e+00
30 40 50 60 70 80
dpi
(b)
AUC (a.u.)
600
500
400
300
200
100
0
b a b b a a
+NP/LNP/-AMF
+NP/LNP/+AMF
-NP/LNP/-AMF
-NP/LNP/+AMF
+NP/HNP/-AMF
+NP/HNP/+AMF
(c)
MGR (%)
200
150
100
50
0
+NP/LNP
-NP/LNP
+NP/HNP

Figure 4